

ONE-LOOP CONTRIBUTIONS OF THE SUPER-PARTNER PARTICLES TO $E^-E^+ \rightarrow W^-W^+$ IN THE MSSM

KAORU HAGIWARA

Theory Group, KEK, Tsukuba, Ibaraki 305-0801, Japan
E-mail: kaoru.hagiwara@kek.jp

SHINYA KANEMURA

Institut für Theoretische Physik der Universität Karlsruhe, D-76128 Karlsruhe, Germany
E-mail: kanemu@physik.uni-karlsruhe.de

YOSHIAKI UMEDA

II Institut für Theoretische Physik der Universität Hamburg, D-22761 Hamburg, Germany
E-mail: umeda@mail.desy.de

One-loop contributions of super-partner particles to W -pair production at e^+e^- collision are discussed in the MSSM. To obtain trustworthy results we test our calculation using three methods: (1) sum rules among form factors which result from the BRS invariance, (2) the decoupling theorem, (3) the high-energy stability. We examine the corrections taking into account constraints from the direct search experiments and the precision data. The results for the sfermion contributions are presented.

1 Introduction

We discuss the one-loop super-partner particle contributions to $e^-e^+ \rightarrow W^-W^+$ in the MSSM. The SM particles have their partners, such as sfermions and inos. We here concentrate on the sfermion one-loop effects¹. The sfermions include squarks and sleptons, whose mass matrices are expressed by

$$M_f^2 = \begin{bmatrix} m_{Q,L}^2 + m_Z^2 c_{2\beta} (T_{fL}^3 - \hat{s}^2 Q_f) + m_f^2 & -m_f A_f^{\text{eff}} \\ -m_f A_f^{\text{eff}*} & m_{U,D,E}^2 + m_Z^2 c_{2\beta} \hat{s}^2 Q_f + m_f^2 \end{bmatrix}.$$

The off-diagonal elements $A_{D,E}^{\text{eff}} = A_{D,E} + \mu \tan \beta$ and $A_U^{\text{eff}} = A_U + \mu \cot \beta$ are multiplied by the fermion mass, so that the mixing are important for stops.

2 Calculation

Helicity amplitudes for $e^-(k, \tau) e^+(\bar{k}, \bar{\tau}) \rightarrow W^-(p, \lambda) W^+(\bar{p}, \bar{\lambda})$, where k, \bar{k}, p, \bar{p} are momenta, $\tau, \bar{\tau} (= -\tau), \lambda, \bar{\lambda}$ are helicities, may be expressed by using 16 basis tensors as

$$\mathcal{M}_\tau^{\lambda\bar{\lambda}} = \sum_{i=1}^{16} F_{i,\tau}(s, t) j_\mu T_i^{\mu\alpha\beta} \epsilon_\alpha^*(p, \lambda) \epsilon_\beta^*(\bar{p}, \bar{\lambda}). \quad (1)$$

The 16 form factors, $F_{i,\tau}$, include all information of the dynamics, while the other part are determined by the kinematics. For physical W -pair production, 9 basis tensors are enough. The rest are used for processes with unphysical (scalar) W bosons, which are used for the test of $F_{i,\tau}$. For this test, we also need to calculate $e^-(k, \tau) e^+(\bar{k}, \bar{\tau}) \rightarrow W^-(p, \lambda) w^+(\bar{p})$ (w^+ : the Nambu-Goldstone boson), whose amplitudes are decomposed as

$$\mathcal{M}_\tau^\lambda = i \sum_{i=1}^4 H_{i,\tau}(s, t) j_\mu S_i^{\mu\alpha} \epsilon_\alpha^*(p, \lambda), \quad (2)$$

with four basis tensors and form factors $H_{i,\tau}$.

We employ the $\overline{\text{MS}}$ scheme, and we take \hat{e}, \hat{g} and M_W as input SM parameters. The MSSM $\overline{\text{MS}}$ couplings are determined by

$$\frac{1}{\hat{e}_{\text{MSSM}}^2(\mu)} = \frac{1}{\hat{e}_{\text{SM}}^2(\mu)} - \Delta\Pi_{T,\gamma}^{QQ}(0, \mu), \quad (3)$$

$$\frac{1}{\hat{g}_{\text{MSSM}}^2(\mu)} = \frac{1}{\hat{g}_{\text{SM}}^2(\mu)} - \Delta\Pi_{T,\gamma}^{3Q}(0, \mu), \quad (4)$$

where $\Delta\Pi_{T,\gamma}^{QQ}(0, \mu)$ and $\Delta\Pi_{T,\gamma}^{3Q}(0, \mu)$ are non-SM contributions to gauge-boson two-point functions. The SM $\overline{\text{MS}}$ couplings are calculated by using the SM RGE's and experimen-

Test by using the BRS sum rule ($i = 1, \tau = -1$)		
\sqrt{s}	Left-hand-side	$\xi_{1j} F_j(s, t)$
	Right-hand-side	$C_{\text{mod}} H_i(s, t)$
200 GeV	$-1.385496590672218 \times 10^{-6}$	$-1.385496590672223 \times 10^{-6}$
1000 GeV	$-6.682526871892199 \times 10^{-8}$	$-6.682526871892053 \times 10^{-8}$

Table 1. The test by the BRS sum rules.

tal values for the effective charges². $M_W = 80.41 \text{ GeV}$ is taken from the data.

3 Tests

One difficulty in loop-level calculations is to determine reliability of the results. This is especially so in our process in which a subtle gauge cancellation takes place among diagrams at each level of perturbation. Incomplete treatment for higher order terms can lead artificially large collections. In order to obtain solid results, we test our calculation by the following methods.

3.1 The BRS invariance

Useful sum rules among form factors between the $W^- W^+$ and the $W^- w^+$ processes are induced from the BRS invariance;

$$\sum_{j=1}^{16} \xi_{ij} F_{j,\tau}(s, t) = C_{\text{mod}} H_{i,\tau}(s, t), \quad (5)$$

where ξ_{ij} are determined by the kinematic parameters and C_{mod} differs from 1 at loop levels. We can use them to test $F_{i,\tau}$. In Table 1, values for both sides in the sum rule are shown. They coincide with each other.

3.2 The decoupling theorem

The cross section should be of the SM prediction in the large sfermion-mass limit. We use this fact to test the overall renormalization factor which cannot be tested by the BRS sum rules. In Figure 1, for large-mass limit ($1/M^2 \rightarrow 0$: M is a scale of SUSY soft-

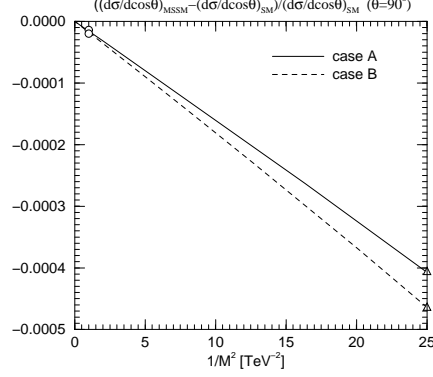


Figure 1. Test of decoupling. Case A and B correspond to non-mixing and stop-mixing cases.

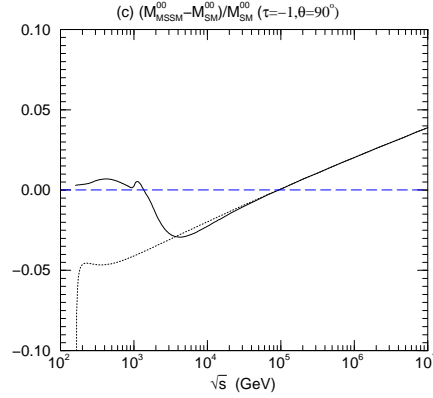


Figure 2. Test for high-energy stability. Real curve and dotted one corresponds to results from the full calculation and the analytic expression, respectively.

breaking masses), the deviation from the SM prediction becomes zero for each case.

3.3 High energy stability

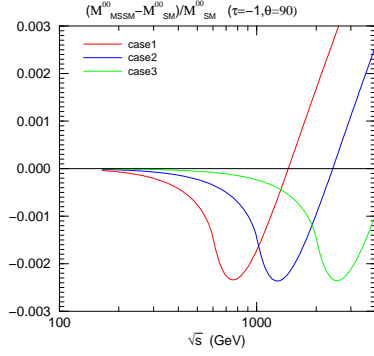
At high energies large gauge cancellation takes place, so it is important to see the high energy stability of the numerical results. We calculate high-energy analytic expression for the amplitude. In Figure 2, the high-energy expression and the full calculation give same results in the high energy limit.

4 Sfermion one-loop effects

In Figure 3, the squark one-loop effects on the 00 helicity amplitude for parameter sets in Table 2. The corrections to the SM predic-

First 2 generations	Case 1	Case 2	Case 3
Input parameters			
$m_{\tilde{Q}} = m_{\tilde{U}} = m_{\tilde{D}}$	300	500	1000
$A_{\tilde{f}}^{eff}$	0	0	0

Table 2. Cases without mixing.

Figure 3. Squark effects of the first two generation. There is no mixing between \tilde{f}_L and \tilde{f}_R

tion are negative and the behavior is rather simple. There is a peak slightly after the squark-pair threshold. The corrections to the SM prediction are at most a few times 0.1%.

In Figure 4, effects of the third generation squarks with large stop-mixing are shown. The parameters defined in Table 3 are chosen so as to be the maximal mixing with mixing angle 45° . The corrections are positive. Larger effects appear for larger A_f^{eff} . It, however, turns out that such enhancement due to the mixing is strongly constrained by the precision data. In Figure 5, each case in Table 3 is plotted on the S - T parameter plane¹. The cases for large corrections (case 2, case 3 in Table 3) stay outside the 99% contour and thus they are excluded. After all only smaller corrections than a few times 0.1% are allowed.

5 Conclusion

The sfermion effects on this process is small.

References

1. S. Alam, K. Hagiwara, S. Kanemura, R. Szalapski, and Y. Umeda, To appear in Phys. Rev. **D**, (hep-ph/0002066), and references therein; Nucl. Phys. **B541** (1999) 50.
2. K. Hagiwara, D. Heitd, C.S. Kim and S. Matsumoto, Z. Phys. **C64** (1994) 559.

$\tilde{t}\text{-}\tilde{b}$ sector:	Case 1	Case 2	Case 3
Input parameters			
$m_{\tilde{Q}} = m_{\tilde{U}} = m_{\tilde{D}}$	300	400	500
$A_{\tilde{f}}^{eff}$	625	1025	1539
Output parameters			
$m_{\tilde{t}_1}$	100	100	100
$m_{\tilde{t}_2}$	478	607	741
$\cos \theta_{\tilde{t}}$	0.708	0.708	0.707

Table 3. Maximal stop-mixing cases.

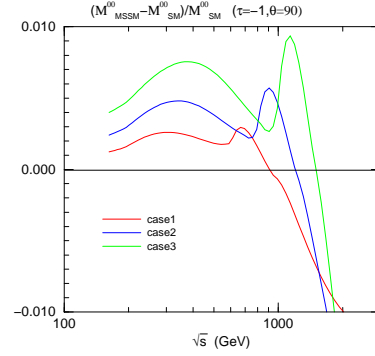
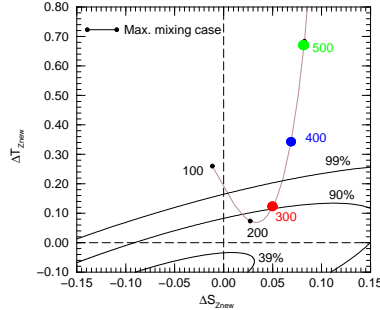


Figure 4. The third-generation squark effects. Maximal stop-mixing cases.

Figure 5. The parameter sets defined in Table 3 on S - T plane. The origin indicates the SM prediction.